microbial biotechnology

Open Access

Proteomic characterization of extracellular vesicles produced by several wine yeast species

Ana Mencher,[1] Pilar Morales,[1] Eva Valero,[2] Jordi Tronchoni,[1,†] Kiran Raosaheb Patil[3,4] and Ramon Gonzalez[1*]

[1]*Instituto de Ciencias de la Vid y del Vino (CSIC, Gobierno de la Rioja, Universidad de La Rioja), Finca La Grajera, Carretera de Burgos, km 6, Logroño, La Rioja 26071, Spain.*

[2]*Universidad Pablo de Olavide, Sevilla, Spain.*

[3]*European Molecular Biology Laboratory, Heidelberg, Germany.*

[4]*The Medical Research Council Toxicology Unit, University of Cambridge, Cambridge, UK.*

Summary

In winemaking, the use of alternative yeast starters is becoming increasingly popular. They contribute to the diversity and complexity of wine sensory features and are typically used in combination with *Saccharomyces cerevisiae*, to ensure complete fermentation. This practice has drawn the interest on interactions between different oenological yeasts, which are also relevant in spontaneous and conventional fermentations, or in the vineyard. Although several interactions have been described and some mechanisms have been suggested, the possible involvement of extracellular vesicles (EVs) has not yet been considered. This work describes the production of EVs by six wine yeast species (*S. cerevisiae*, *Torulaspora delbrueckii*, *Lachancea thermotolerans*, *Hanseniaspora uvarum*, *Candida sake* and *Metschnikowia pulcherrima*) in synthetic grape must. Proteomic analysis of EV-enriched fractions from *S. cerevisiae* and *T. delbrueckii* showed enrichment in glycolytic enzymes and cell-wall-related proteins. The most abundant protein found in *S. cerevisiae*, *T. delbrueckii* and *L. thermotolerans* EV-enriched fractions was the enzyme exo-1,3-β-glucanase. However, this protein was not involved in the here-observed negative impact of *T. delbrueckii* extracellular fractions on the growth of other yeast species. These findings suggest that EVs may play a role in fungal interactions during wine fermentation and other aspects of wine yeast biology.

Received 31 March, 2020; accepted 31 May, 2020.
*For correspondence. E-mail rgonzalez@icvv.es; Tel. +34 941 89 49 80; Fax +941 89 97 28.
†Present address: Universidad Internacional de Valencia, Valencia, Spain.
Microbial Biotechnology (2020) **13**(5), 1581–1596
doi:10.1111/1751-7915.13614
Funding information
This work was funded by the Spanish Government through grants AGL2015-63629-R (co-financed by FEDER funds), PCI2018-092949 (co-funded by ERA-CoBioTech) and BES-2016-077557 (training contract for AM). JT is funded by FGCSIC by the COMFUTURO program.

Introduction

Extracellular vesicles (EVs) are particles naturally released from living cells and delimited by a lipid bilayer that cannot self-replicate (Théry *et al.*, 2018). They are produced by organisms belonging to all three domains of the tree of life and show a broad range of sizes, from 20 to 500 nm, depending on biological species, cell types and environmental conditions. They can be produced by various mechanisms and have historically received different names, depending on the organism of origin or the biogenesis pathway. However, in the absence of clear evidence of the mechanism of release, the generic term extracellular vesicle is recommended (Théry *et al.*, 2018).

Mammalian cells produce different types of EVs, including secretory lysosomes, multi-vesicular body-derived exosomes or microvesicles (Nickel and Rabouille, 2009; Rabouille *et al.*, 2012). Mammalian EVs have been widely studied because they are involved in multiple biological events such as antigen presentation, neuronal communication, viral transmission, immune modulation, tumour angiogenesis or metastasis (Raposo *et al.*, 1996; Marzesco *et al.*, 2005; Bhatnagar *et al.*, 2007; Park *et al.*, 2010). EV research on other biological systems (bacteria, plants, fungi) is a younger but growing field (Regente *et al.*, 2009; Brown *et al.*, 2015). EV morphology and content (including peptides, proteins, miRNAs or mRNAs) have been analysed for several yeast species, mostly pathogenic (Rodrigues *et al.*, 2007; Rodrigues *et al.*, 2014; Gil-Bona *et al.*, 2017; Rodrigues and Casadevall, 2018). Both non-conventional and conventional secretory proteins have been identified on yeast EVs (Gil-Bona *et al.*, 2015). Fungal EVs have been involved in cell-to-cell communication, response to nutrient availability, RNA export, morphological transition

(e.g. biofilm formation), prion transmission, modulation of host immunity, cell wall remodelling, or survival to stress conditions (Oliveira *et al*., 2013; Peres da Silva *et al*., 2015; Rizzo *et al*., 2017; Zhao *et al*., 2019). However, in most cases, the attribution of functions or biological roles to fungal EVs is supported by few or single examples, and the mechanisms or cause–effect relationships are not well established.

The relevance of EVs for the biotechnological application of yeasts remains unexplored. Food fermentation often develops as mixed culture, including wine, kefir, sourdough and other foods (Farnworth, 2005; Manzanares *et al*., 2011; Furukawa *et al*., 2013; De Vuyst *et al*., 2014; Jouhten *et al*., 2016). In addition, there is a current trend in winemaking for the use of multiple (usually two or three) yeast starter cultures, from different yeast species in order to reach specific quality and compositional outcomes (Gonzalez *et al*., 2013; Jolly *et al*., 2014).

Many of the interactions observed between wine microorganisms can be considered as indirect. This would be the case for competition for the absorption of nutrients (Fleet, 2003) or to the toxic effect of major metabolites, such as ethanol (Kunkee, 1984). But direct or targeted mechanisms of interaction might be just as important in many instances. For example, killer factors have been described in both *Saccharomyces* (Van Vuuren and Jacobs, 1992; Pérez *et al*., 2001; Rodríguez-Cousiño *et al*., 2011) and non-*Saccharomyces* species such as *Torulaspora delbrueckii* (Velázquez *et al*., 2015). Interestingly, peptide fragments from GAPDH, a glycolytic enzyme, secreted by *S. cerevisiae*, show antimicrobial activity against several wine microorganisms (Branco *et al*., 2014). In addition, Rossouw *et al.,* (2018) showed the impact of physical contact on population dynamics, and several studies suggest a role of cell-to-cell contact on wine yeast interspecific interactions (Taillandier *et al*., 2014; Wang *et al*., 2015; Pérez-Torrado *et al*., 2017; Englezos *et al*., 2019; Shekhawat *et al*., 2019). Finally, quorum sensing mechanisms have been described for some yeast species (Chen and Fink, 2006).

Some insight on the mechanisms involved in interactions between wine yeasts was provided by transcriptomic analysis (Tronchoni *et al*., 2017; Curiel *et al*., 2017). These authors found transcriptional reprogramming, suggesting activation of nutrient consumption pathways by *S. cerevisiae* in response to several wine yeast species. Considering the short response time, transcriptional reprogramming was likely mediated by specific recognition mechanisms. Recently, similar results have been reported by other authors (Shekhawat *et al*., 2019; Alonso del Real *et al*., 2019).

As a follow-up of previous studies on interspecific yeast interactions in winemaking, and considering the multiple roles already attributed to fungal EVs, including biological communication (Stahl and Raposo, 2018; Raposo and Stahl, 2019), we posed the hypothesis that EVs would be involved in, at least, some of the responses to co-cultivation observed among wine yeasts. In this work, we show that EVs are indeed produced by several wine yeast species under cultivation conditions relevant for winemaking and perform a proteomic analysis of the extracellular fractions of the two more relevant wine yeast species.

Results

Production of extracellular vesicles by wine yeast species

Fractions from cell-free supernatants, enriched in either extracellular vesicles or free extracellular proteins, were isolated as described under Experimental procedures. They were labelled as EV-enriched fractions (for extracellular vesicles) or VF-enriched fractions (for vesicle-free), and were obtained from two *S. cerevisiae* strains (EC1118 and FX10) and five non-*Saccharomyces* yeasts (*T. delbrueckii, Hanseniaspora uvarum, Candida sake, Metschnikowia pulcherrima* and *Lachancea thermotolerans*), growing in synthetic grape must. Cell viability was quantified by flow cytometry in order to rule out contamination by cytoplasmic proteins released by dead or lysed cells. According to this criterion, the 24-hour sampling point was selected for the analyses. At this sampling point, the number of dead cells was below 2% for all yeast strains.

The EV-enriched fractions were prepared and visualized by TEM with negative staining (see Experimental procedures). EVs were observed for all seven yeast strains. Intact EVs showed a white (stain free) perimeter, corresponding to the membrane of the vesicle, while the lumen was dark due to stain absorption. Additionally, the footprints of other EVs were appreciated as clear haloes over the darker background of the negative staining preparations. They were spherical or ovoid in shape (Fig. 1) and showed a size range around 100-200 nm in diameter. Size variability for each strain was roughly $\pm$ 50%. The smallest average diameter was shown by *L. thermotolerans* (105 nm) and *H. uvarum* (111 nm), and the larger one by *C. sake* (204 nm). EVs from *M. pulcherrima* showed the widest size distribution among all the species tested. EVs produced by the two *S. cerevisiae* strains showed similar size distributions (Fig. 1).

Proteome composition of S. cerevisiae *and* T. delbrueckii *EV- and VF-enriched fractions*

To better understand the biological impact of EVs on wine yeast biology, the proteome composition of EV- and VF-enriched fractions was analysed. Considering

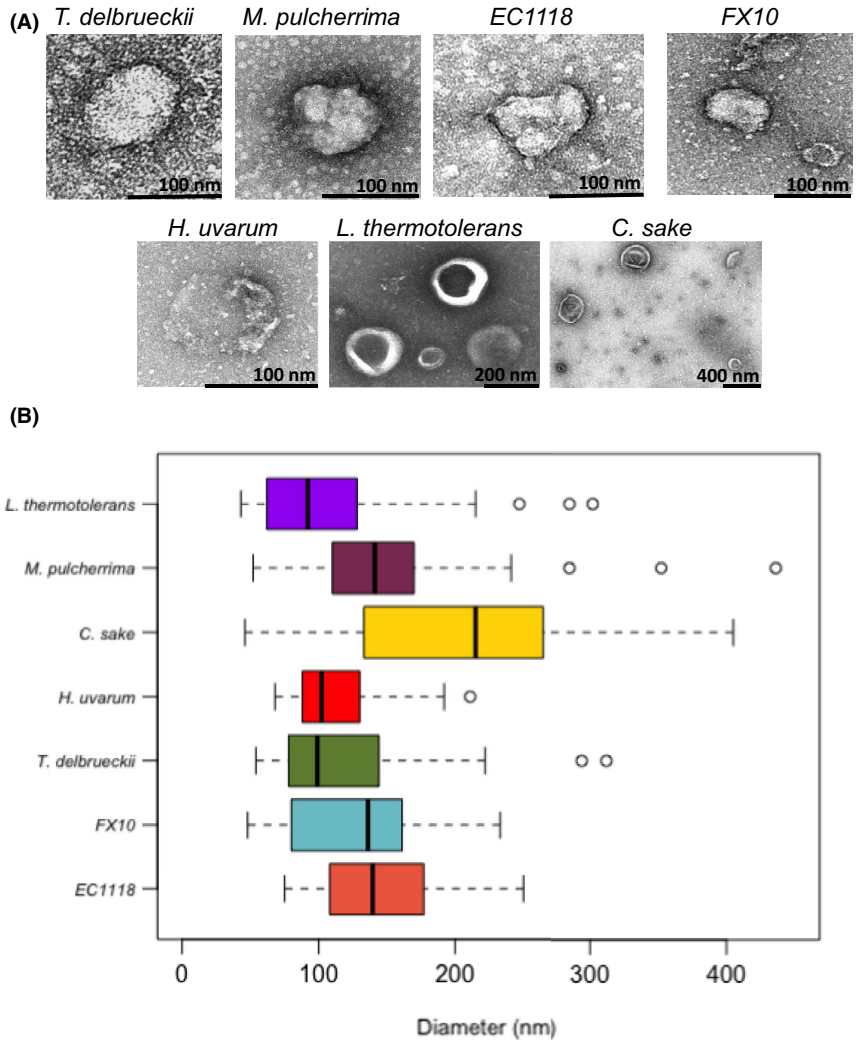

Fig. 1. TEM (negative staining) of EV-enriched fractions of different wine yeast strains grown in synthetic grape must (A), and box plot showing the size distribution of the EVs on these samples (B).

their relevance as starter cultures, as well as the availability of suitable protein data bases, *S. cerevisiae* (EC1118) and *T. delbrueckii* were selected for proteomic analysis.

After processing raw data, 61 and 72 proteins passing the filtration criteria (see Experimental procedures) were identified in the VF-enriched fractions of *S. cerevisiae* and *T. delbrueckii,* respectively (Table S1). These proteins were classified into four groups (Fig. 2): cell-wall-related, membrane-related (including permeases), other proteins and uncharacterized proteins. Cell-wall-related group was the most abundant protein group in the VF-enriched fractions for both *S. cerevisiae* and *T. delbrueckii*, with 32 and 28 proteins, respectively, while the membrane-related group was represented by just 7 or 11 proteins (for *S. cerevisiae* and *T. delbrueckii,* respectively). Analysis of *S. cerevisiae* VF proteins in the STRING database showed a glycolysis-related cluster and a cell-wall-related cluster (Fig. 3). This cluster includes several GPI-anchored yapsin family proteases, which are involved in cell wall growth and maintenance, as well as some of their substrates. The relevance of these clusters was confirmed by the enrichment (above 10-fold, with FDR below 0.01) of biological process GO terms like 'cell wall organization or biogenesis', 'glucose metabolic process', or 'glycolytic process' and related terms (Table S2). A similar picture, i.e. predominance of cell-wall-related proteins arose from the analysis of *T. delbrueckii* VF proteins (Fig. 3), also confirmed by enrichment of 'cell wall organization or biogenesis' and similar or related terms (Table S2). In this case, and despite some glycolytic enzymes were identified, the glycolysis-related cluster was less individualized, and no cognate enriched terms were found.

On the other side, the number of different proteins identified from the EV-enriched fraction was 35 for *S. cerevisiae* and 33 for *T. delbrueckii* (Table S1). Proportions between the three defined categories were similar to VF fraction in the case of *S. cerevisiae* (54% cell-wall-related, 12% membrane-related and 34% other proteins). However, in *T. delbrueckii* the percentage of cell-wall-related proteins in EV-enriched fraction increased as compared to the VF-enriched fraction (from 39% to 52%), at the expenses of the 'other proteins' (Fig. 2). EV proteins of *S. cerevisiae* were grouped by STRING into two well-defined clusters (Fig. 3), one related to glucose metabolism and the other to cell wall metabolism, highlighted by the same GO biological process as for VF proteins: 'cell wall organization or biogenesis', 'glucose metabolic process' or 'glycolytic process' (Table S2). A cell-wall-related cluster was also observed for *T. delbrueckii* EV proteins (Fig. 3), but the glucose utilization related cluster almost disappeared (represented by just Cdc19 and Eno1). In contrast, *T. delbrueckii* proteins in the EV-enriched fraction showed a cluster of three proteins involved in iron assimilation. Several iron-related categories were enriched in this data set, including 'reductive iron assimilation' and 'iron ion transport' (Table S2).

Proteins in these fractions were also screened for predicted secretory signal peptide or GPI anchor in the primary sequence, as described under Experimental procedures. Above two thirds of the proteins (69–77%) were found to be classical secretion proteins in each of the four data sets (Table S1). There was no enrichment in non-canonical secretion proteins for the EV-enriched fractions. Also, similar proportions of putative GPI-anchored proteins (23–28%) were obtained for most data sets, apart from EVs from *T. delbrueckii*, with only 12% of GPI-anchored proteins (Table S1). No significative enrichment in classical secretion or GPI-anchored proteins was found, either, by selecting the most abundant proteins (data not shown).

In addition to qualitative presence, protein abundance is an important feature to understand the biological significance of the proteins detected in EV- and VF-enriched fractions. According to normalized relative spectral abundance counting factor (NSAF) values, exo-1,3-β-glucanase (Exg1 in *S. cerevisiae*) was the most abundant protein in three of the four data sets (Fig. S1). It represented around 14% and 31% of protein abundance for *S. cerevisiae* and *T. delbrueckii* VF-enriched fractions, respectively, and 23% and 14% in *S. cerevisiae* and *T. delbrueckii* EV-enriched fractions. On average, abundance of Exg1 was 2.7 times higher than the second more abundant protein, Bgl2, also related with the cell wall. About half of the most abundant proteins were shared among the four data sets (Fig. S1). Most of these shared proteins are cell-wall related. The two exceptions are Kar2, involved in protein import into the ER and the unfolded protein response, and the glycolytic enzyme Eno1. However, Kar2 was only abundant for the *T. delbrueckii* EV fraction. On the other side, the number

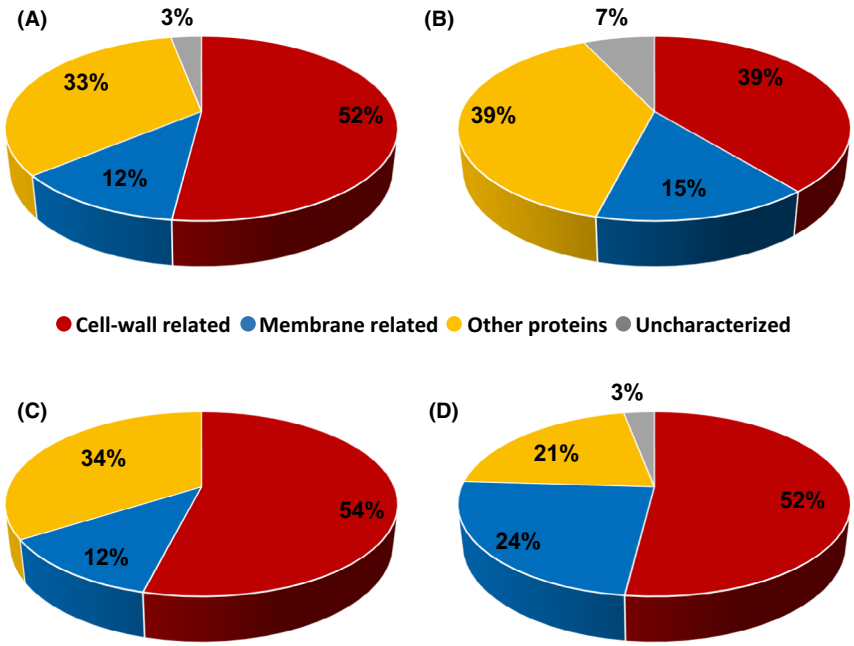

Fig. 2. Categorization of the proteins identified in different yeast extracellular fractions. *S. cerevisiae* VF-enriched fraction (A), *T. delbrueckii* VF-enriched fraction (B), *S. cerevisiae* EV-enriched fraction (C), and *T. delbrueckii* EV-enriched fraction (D).

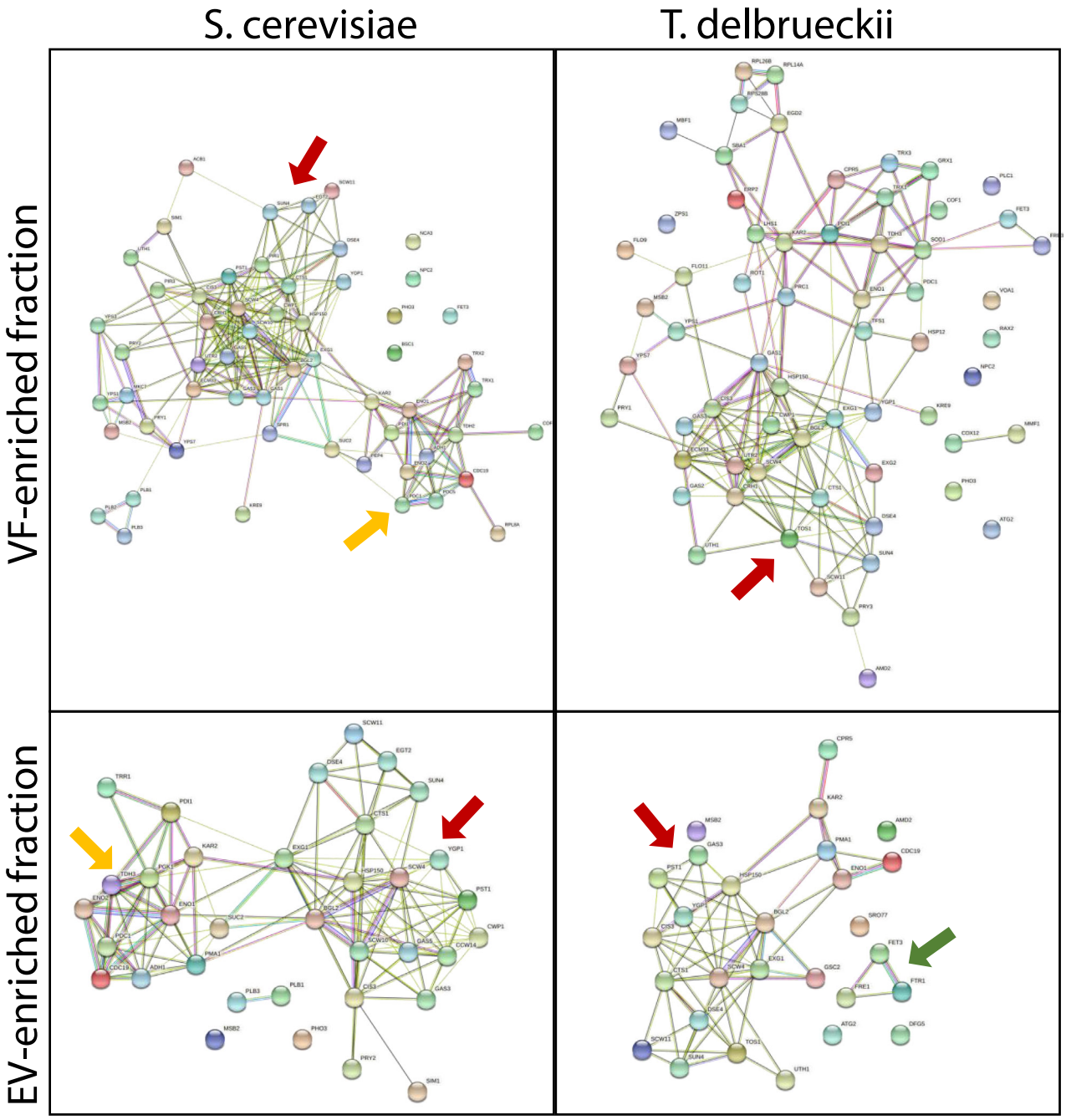

Fig. 3. Known interaction networks between the proteins present in *S. cerevisiae* and *T. delbrueckii* VF- and EV-enriched fractions, identified with STRING database. Red arrows indicate the cell wall organization- or biogenesis-related clusters, yellow arrows indicate the glucose utilization-related cluster, and the green arrow indicates a cluster of three proteins involved in iron assimilation.

of Eno1 peptides is high in the EV fractions (especially for *S. cerevisiae*), but much lower for the VF fraction. Pma1, the major plasma membrane H^+-ATPase, is found in EVs of both yeast species, but not in the VF fractions.

Comparison of proteins found in the equivalent fraction (EV or VF) for each species showed an important overlapping. In both cases, about 50% of the proteins identified for *S. cerevisiae* were also found in *T. delbrueckii*, and *vice versa* (Fig. 4). Oliveira *et al.* (2010) analysed the EV protein content of several wild-type and mutant *S. cerevisiae* strains growing on Sabouraud dextrose medium. About two thirds (21 proteins) of the

proteins found in *S. cerevisiae* EVs in the present work were also found by them in EVs (data not shown). This includes all the enzymes in the data set involved in glucose catabolism (Eno1, Eno2, Tdh3, Pdc1, Adh1, Cdc19, Pgk1), as well as many of those related to the cell wall metabolism.

In addition, major proteins in EV-enriched fractions were confirmed by SDS-PAGE with Coomassie blue staining, along with other fractions from the purification process. A common feature of the EV-enriched fraction of *L. thermotolerans*, *T. delbrueckii*, and the two strains of *S. cerevisiae* was a prominent band about 45-50 kDa in size (Fig. S2). Peptide mass fingerprinting clearly identified them as Exg1 in both *S. cerevisiae* strains, or the probable ortholog proteins from the other two species (Table 1). This result confirmed the finding of exo-1,3-β-glucanase being a major protein constituent of *S. cerevisiae* and *T. delbrueckii* EVs, supported by proteomic analysis, but it also extends this feature to other wine yeast species.

Evaluation of Exg1 as a potential inducer of cell death on target yeasts

Exo-1,3-β-glucanases are fungal cell-wall-degrading enzymes. They play an essential role in cell wall remodelling (Ene *et al.*, 2015), required for cell growth and division, but they are also used as biological weapons by some mycoparasitic organisms (Schaeffer *et al.*, 1994; Jiang *et al.*, 2017). This led us to the hypothesis that Exg1 found in the extracellular fractions of these yeasts might be involved in antagonistic interactions. The effect of cell-free supernatants containing Exg1 (i.e. from *T. delbrueckii*, *L. thermotolerans*, and the two strains of *S. cerevisiae*) was tested against *H. uvarum* and *S. cerevisiae* FX10, as described under Experimental procedures. These target yeasts were selected according to a preliminary experiment in which *T. delbrueckii* EVs had shown inhibitory activity (not shown). Growth on synthetic grape must in microwell plates was monitored by flow cytometry at different time points. Both target yeasts showed reduced growth in the presence of *T. delbrueckii* cell-free supernatants, resulting in viable cell numbers below 50% of the control after 14, 17 or 24 h of incubation (Fig. 5). These cultures also contained about three times more dead cells than the control at the different time points. This result shows that supernatants from *T. delbrueckii* hinder yeast growth by inducing death of *S. cerevisiae* and *H. uvarum* cells. The involvement of Exg1 in this activity was tested by two complementary approaches. First, 24-hour cell-free supernatants of a collection of 31 additional *T. delbrueckii* isolates were screened for the induction of cell death in *S. cerevisiae* FX10. The ability to induce cell death in *S. cerevisiae* was found to be strain specific. Indeed, only 13% of the strains showed this feature (Fig. S3). In contrast, the Exg1 band was detected in all these cell-free supernatants (data not shown), indicating a lack of correlation between the presence of Exg1 and growth inhibition.

The second approach consisted of the construction of a recombinant *T. delbrueckii* strain defective for exo-1,3-β-glucanase (gene code: Tdel_0G03720). Gene deletion was confirmed in three ways. First, the 5′ edge and whole region were amplified by PCR, and the expected

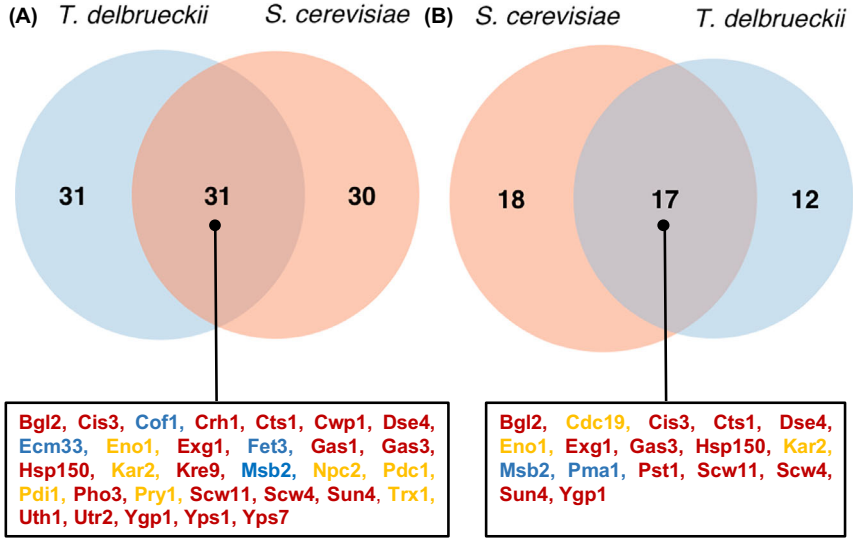

Fig. 4. Venn diagrams showing the shared proteins identified in *S. cerevisiae* and *T. delbrueckii* VF-enriched (A) or EV-enriched (B) fractions. Cell-wall-related proteins are shown in red characters; those related to the cell membrane in blue; and the group of 'other proteins' in yellow characters.

Table 1. Mascot Proteome Discoverer results for the major protein (excised from SDS-PAGE gels) found in the EV-enriched fractions from *S. cerevisiae* (FX10 and EC1118), *T. delbrueckii* and *L. thermotolerans*.

Yeast	Name of the protein ('closest match')	Closest homology	Molecular function	Biological process	Molecular mass (Mr)	Isoelectric point (pI)	Sequence coverage
S. cerevisiae EC1118	Exg1p		Exo-1,3-beta-glucanase	Cell wall beta-glucan metabolic process	51.7 kDa	4.57	0.61
S. cerevisiae FX10	Exg1p		Exo-1,3-beta-glucanase	Cell wall beta-glucan metabolic process	51.7 kDa	4.57	0.66
T. delbrueckii	hypothetical protein TDEL_0G03720	Exg1p de S.c (S288c)	O-glycosyl hydrolase	Carbohydrate metabolic process	51.2 kDa	4.66	0.49
L. thermotolerans	KLTH0H06974p		Endo-1,6-beta-glucosidase	Cell wall beta-glucan metabolic process	51.0 kDa	4.69	0.53

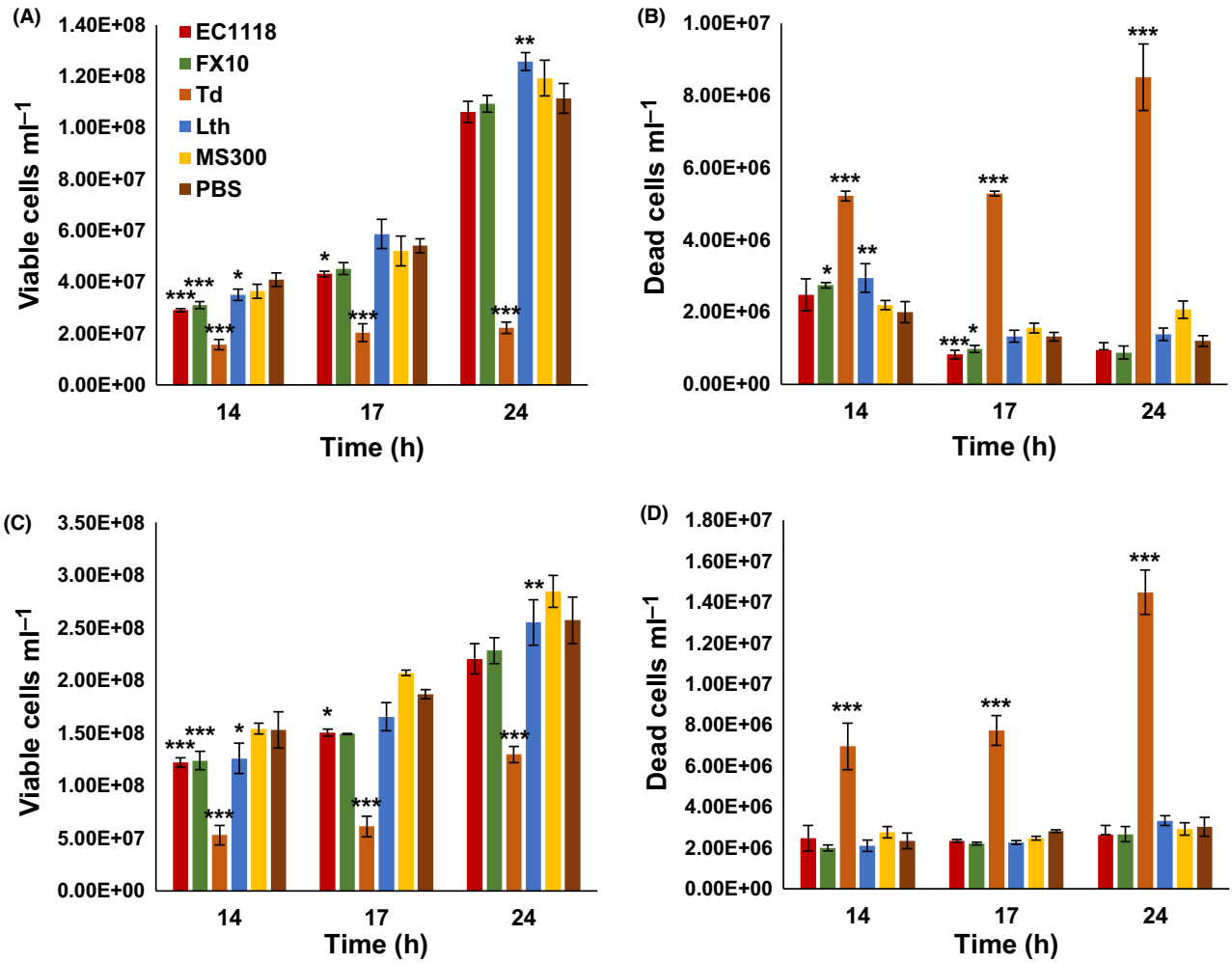

Fig. 5. Effect of 24-h cell-free supernatants from two *S. cerevisiae* strains: EC1118 and FX10; and two non-*Saccharomyces* yeasts: *T. delbrueckii* (*Td*) and *L. thermotolerans* (*Lth*), on growth and viability of two target yeast strains: FX10 (A and B), and *H. uvarum* (C and D). MS300 and PBS were used as negative controls. Confidence bars represent standard deviation measures. Statistically significant differences with the PBS control, within each time point, are indicated by *, ** or *** for *P*-values ≤ 0.05, ≤ 0.01 or ≤ 0.001, respectively.

amplicon sizes were obtained. Then, two of the putative deletion strains were confirmed to have lost enzyme activity. Finally, the disappearance of the cognate protein band was established by silver-stained SDS-PAGE analysis. Details are shown in Figure S4. The ability to inhibit growth of *S. cerevisiae* and *H. uvarum* was tested for the two deletion strains in comparison with suitable positive and negative controls. Growth inhibition and induction of cell death were identical for the cell-free supernatants of the wild-type and the exo-1,3-β-glucanase defective *T. delbrueckii* deletion strains (Fig. 6).

Discussion

Interaction mechanisms and cell-to-cell communication between wine yeasts have drawn the attention of many wine biotechnologists during the past ten years. Researchers have explored antagonistic and synergistic behaviours concerning cell growth and fermentation kinetics, based on competition for substrates, release of inhibitors, and cell-to-cell contact, among other mechanisms. Other cell-to-cell communication mechanisms, namely quorum sensing molecules, have been explored for *S. cerevisiae* as well as non-*Saccharomyces* wine yeasts (Chen *et al*., 2004; González *et al*., 2018). However, the relevance of EVs in this context remained unexplored. All the wine yeast species studied in this work produced extracellular vesicles that could be visualized by electron microscopy. It should be noted that these vesicles were purified from cultures in synthetic grape must, not standard laboratory media. Therefore, it is expected that they will produce EVs also in real winemaking conditions or in the vineyard. The protein content of EVs is not a simple mirror of all the proteins secreted by the cells in culture, even though a relevant percentage of the proteins detected in EVs are also found in the VF fraction, and no enrichment on non-conventional secretory proteins was found for EV-enriched fractions (according to data from signal peptide and GPI anchor *in silico* identification). These data are in accordance with those reported for similar fractions from different fungal species (Oliveira *et al*., 2010; Vallejo *et al*., 2012; Rodrigues *et al*., 2014; Gil-Bona *et al*.,

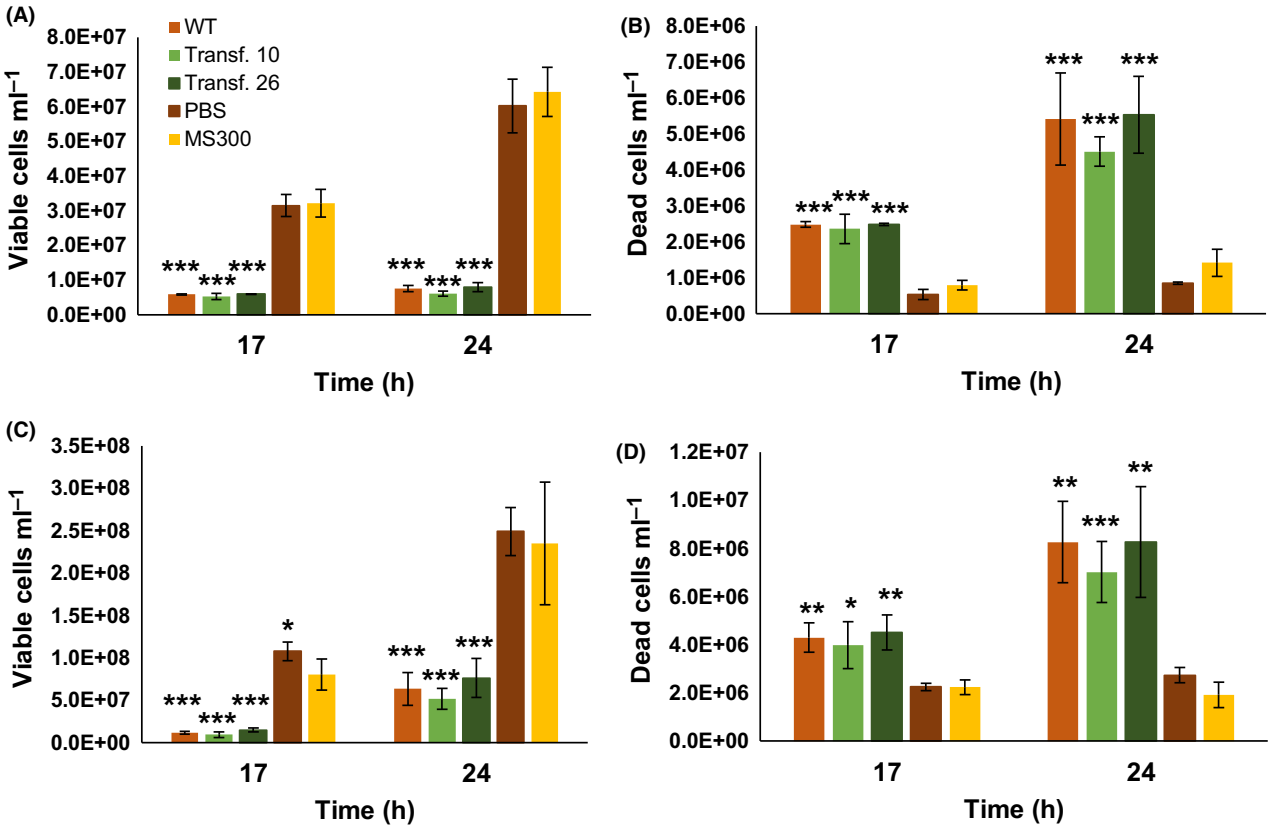

Fig. 6. Effect of 24-h cell-free supernatants from two knock-out selected strains, compared to the original strain of *T. delbrueckii,* on the growth and viability of two target yeast strains: FX10 (A and B), and *H. uvarum* (C and D). MS300 and PBS were used as negative controls. Confidence bars represent standard deviation measures. Statistically significant differences with the PBS control, within each time point, are indicated by *, ** or *** for *P*-values ≤ 0.05, ≤ 0.01 or ≤ 0.001, respectively.

2015). It is currently assumed that many of these non-classical secretory proteins reach the extracellular space by several alternative pathways (Oliveira *et al*., 2010; Miura *et al*., 2012; Miura and Ueda, 2018; Winters *et al*., 2020). However, it cannot be excluded that some of the proteins found in the soluble fraction of the secretome reached the extracellular space as vesicle-associated, being released from those structures after crossing the cell wall, or during the purification process.

Also noteworthy is the similarity in protein content between different yeast species. Relevant similarities in EV protein content have been previously reported among pathogenic fungal species. Since *S. cerevisiae* and *T. delbrueckii*, the two species analysed in more depth in this work, are relatively close in the phylogenetic tree, the extent of this similarities among wine yeast species cannot be predicted, but the fact that the major protein found in *L. thermotolerans* was also an ortholog of Exg1, the major protein found in the other two species, should be taken into account. Indeed, Exg1 was also found by other authors in *C. albicans* and other fungal EVs.

The presence of glycolytic enzymes in the extracellular fractions might be surprising at first sight. However, glycolytic enzymes are frequently reported in EV preparations from different yeast (Rodrigues *et al*., 2014; Gil-Bona *et al*., 2015) or bacterial (Hong *et al*., 2019) species, and some human exosomes have been shown to be able to synthesize ATP by glycolysis, suggesting ATP production might play a role in the uptake of extracellular vesicles by target cells (Fonseca *et al*., 2016). Indeed, enolase has been found in EVs from most yeast species analysed so far (Rodrigues *et al*., 2014), including *S. cerevisiae* and *T. delbrueckii* in the present work, which might be related to the moonlighting character of this protein (Decker and Wickner, 2006; Gancedo and Flores, 2008), involved for example in vacuolar membrane fusion. This might indicate a specific role of this protein in the biology of fungal EVs. The glycolytic enzyme GAPDH, identified as two different isoenzymes, Tdh2 and Tdh3, in the VF- and EV-enriched fractions (respectively) of *S. cerevisiae* has also a moonlighting character; peptide fragments of this enzyme show inhibitory activity against other yeasts and bacteria (Branco *et al*., 2014).

Furthermore, enzymes related to cell wall architecture have been often found in the EV-associated proteome of *C. albicans* (Vargas *et al*., 2015; Gil-Bona *et al*., 2015) or *S. cerevisiae* (Oliveira *et al*., 2010; Zhao *et al*., 2019) and other fungal species (Baltazar *et al*., 2016). The problem of fungal EV passage of the cell wall has been raised since the origins of research in this field (Wolf and Casadevall, 2014). Some authors have suggested a potential relationship between the cell wall remodelling activities of these enzymes and the passage of extracellular vesicles across this otherwise rigid structure (Oliveira *et al*., 2010; Wolf and Casadevall, 2014; Gil-Bona *et al*., 2015). However, available studies do not allow to fully ascertain the relevance of these enzymatic activities on the mechanism of extracellular vesicle release by fungal species. Finally, Pma1 contains 10 transmembrane domains, which may explain its absence from the soluble fraction. It was also found in vesicles from other yeast species, and its presence was taken as an indication that EVs might be derived, at least partially, from the plasma membrane (Vallejo *et al*., 2012; Gil-Bona *et al*., 2015), although the exact mechanism has not yet been established and the co-occurrence of several biogenesis pathways for fungal EV formation is almost a consensus (Oliveira *et al*., 2010; Miura and Ueda, 2018; Zhao *et al*., 2019).

Possible involvement of Exg1 on antagonistic interactions was ruled out in two ways. First, supernatants from a collection of *T. delbrueckii* strains contained this protein band independently of the inhibitory effect on other yeasts. Second, for a *T. delbrueckii* strain showing antagonistic activity, it was unaltered after deletion of the cognate gene. Anyway, the antagonistic interactions of this strain of *T. delbrueckii* with other yeast species highlight the interest of studying the compatibility between yeast strains for a sound design of multiple-starter fermentation processes.

In conclusion, this is the first study targeting EVs in a food biotechnological context. The six wine-related yeast species analysed showed the production of extracellular vesicles under conditions mimicking winemaking conditions. The extracellular fractions (EV or VF enriched) from *T. delbrueckii* and *S. cerevisiae* showed a protein composition reminiscent of that described for other yeast species under different culture conditions, including the abundance of cell-wall-related proteins and glycolytic enzymes. This is the first report of EV production for most of these yeast species (apart from *S. cerevisiae*), the first report of EV production under winemaking conditions, and the first proteomic analysis of EVs from *T. delbrueckii*. Results suggest these extracellular structures might play a relevant role in wine yeast biology and warrant further attention. Exg1 was found as one of the most abundant proteins, not only in the extracellular fractions of *S. cerevisiae* and *T. delbrueckii*, but also for *L. thermotolerans*. However, it could not be related to antagonistic interactions. Next steps to improve our understanding of the role of EVs in wine yeasts biology may involve a deeper biochemical analysis of EVs (e.g. microRNA or lipid content); studying the impact of different culture conditions, including co-cultivation, on the composition of EVs; or analysing the physiological impact of purified EVs on target yeast cultures, not just

considering growth kinetics and cell viability, but using omics approaches (transcriptomics, metabolomics or proteomics).

Experimental procedures

Strains and growth conditions

The following wine *S. cerevisiae* strains were used in this work EC1118 (Lallemand), FX10 (Laffort, SA). Non-*Saccharomyces* yeasts included *T. delbrueckii* CECT 11199 (CBS 1146), *H. uvarum* CECT 10389, *M. pulcherrima* CECT 11202, *C. sake* CECT 11909; as well as yeasts from the culture collection of the ICVV Microwine group (PRICVV collection) *L. thermotolerans* PRICVV905, and 31 T. *delbrueckii* wine strains isolated from vineyard and winemaking environments (PRICVV7, PRICVV9, PRICVV29, PRICVV30, PRICVV34, PRICVV601, PRICVV814, PRICVV815, PRICVV820, PRICVV821, PRICVV846, PRICVV851, PRICVV858, PRICVV873, PRICVV885, PRICVV904, PRICVV925, PRICVV931, PRICVV1008, PRICVV1012, PRICVV1023, PRICVV1095, PRICVV1097, PRICVV1117, PRICVV1118, PRICVV119, PRICVV1120, PRICVV1121, PRICVV1122, PRICVV1123, PRICVV1124). Pre-cultures were grown in YPD medium (1% yeast extract, 2% peptone, 2% glucose) for 48 h at 25°C in static tubes. In order to mimic wine fermentations, yeast cells were cultured in synthetic grape must MS300 (Bely *et al*., 1990) containing (per litre): 100 g glucose; 100 g fructose; 5 g malic acid; 0.5465 g citric acid·H_20; 3 g tartaric acid; minerals (0.75 g KH_2PO_4; 0.5 g K_2SO_4; 0.25 g $MgSO_4·7H_20$; 0.16 g $CaCl_2·2H_2O$; 0.2 g NaCl); 0.46 g total YAN NH_4Cl (120 mg N l^{-1}); 10 ml total YAN Amino acids (288.3 mg N l^{-1}) (Tyr 1.95 g; Trp 17.50 g; Ile 3.25 g; Asp 4.42 g; Glu 11.95 g; Arg 44.5 g; Leu 4.80 g; Thr 7.54 g; Gly 1.82 g; Gln 49.92 g; Ala 14.56 g; Val 4.42 g; Met 3.12 g; Phe 3.77 g; Ser 7.80 g; His 4.57 g; Lys 2.11 g; Cys 2.705 g; Pro 59.93 g, diluted in Na_2CO_3 2%); 1 ml trace elements from a 1000× stock solution ($MnSO_4·H_2O$ 4 g; $ZnSO_4·7H_2O$ 4 g; $CuSO_4·5H_2O$ 1 g; KI 1 g; $CoCl_2·6H_2O$ 0.4 g; H_3BO_3 1 g; $(NH_4)_6Mo_7O_{24}·4H_2O$ 1.0618 g); 10 ml vitamins from a 100× stock solution (Myo-inositol 2 g; pantothenate calcium 0.15 g; Tthiamine hydrochloride 0.025 g; Nicotinic acid 0.2 g; pyridoxal 5′ phosphate·H_2O 0.0365 g; biotin 3 ml); 1 ml anaerobiosis factors from a 1000× stock solution (Ergosterol 1.5 g; Na-Oleate 0.485 g; Tween 80 50 ml, diluted in 100 ml ethanol); pH = 3.3 (adjusted with 10 N NaOH). Flasks of 500 ml containing 200 ml of MS300 were inoculated to an initial OD_{600} of 0.2 and incubated at 25°C, during 24 h with gentle rotary shaking (110 rpm). Depending on the strain, the OD_{600} of MS300 cultures at sampling time ranged from 5.5 to 8.1.

Preparation of extracellular vesicle (EV)- and vesicle-free (VF)-enriched fractions

EV-enriched fractions were isolated from seven yeast strains: *S. cerevisiae* EC1118, *S. cerevisiae* FX10, *T. delbrueckii* CBS1146, *C. sake* CECT 11909, *H. uvarum* CECT 10389, *M. pulcherrima* CECT 11202, and *L. thermotolerans* PRICVV905, as described by Gil-Bona *et al*. (2015). A tablet of protease inhibitors (complete mini, EDTA-free, Roche) was used per litre of culture, and all the steps were carried out at 4°C. Vesicles were obtained from three fully independent cultures per yeast strain. Briefly, yeast cells and debris were removed by two sequential centrifugation steps; first at 5200 g for 15 min and then at 15 000 *g* for 30 min. The cell-free supernatant was collected and filtrated by 0.22 μm using the Thermo Scientific Nalgene Disposable Filter Unit and then concentrated using a 100-kDa Macrosep (Pall Corporation). The concentrated culture was centrifuged again at 15 000 *g* for 30 min to remove smaller debris. The EV-enriched fraction was then recovered by ultracentrifugation in 6.0 ml PC Thick-Walled Tubes (16 × 59 mm; Thermo Fisher Scientific) at 45 000 r.p.m. for 1 h at 4°C in Microultracentrifuge Sorvall™ MTX150 with S80-AT3 fixed angle rotor (Thermo Fisher Scientific). Depending on the use, pellets from ultracentrifugation were washed once under the same conditions and resuspended in 0.5 M triethylammonium bicarbonate (TEAB) for proteomic analysis, or in phosphate-buffered saline (PBS) for TEM or functional studies. Final concentration factor of the EV-enriched fraction was 50 times. For TEM analysis, the final resuspension buffer contained 2% (w/v) paraformaldehyde. Flow-through of the 100-kDa filter and the supernatant recovered from the first ultracentrifugation step were pooled and concentrated by ultrafiltration through a 10-kDa cut-off filter to obtain the VF-enriched fraction. Finally, for the proteomic analysis, the EV-enriched fraction was concentrated with a Genevac™ miVAC DNA Vacuum-Integrated Centrifugal Concentrator System, and the VF-enriched fraction was freeze-dried.

Transmission electron microscopy (TEM)

EV-enriched fractions resuspended in 2% paraformaldehyde in PBS as described above were fixed for 15 min at room temperature and stored at 4°C until TEM analysis. The samples were adsorbed for 10 min to collodion-carbon-coated grids by floating the grids on 10 μl drops on parafilm. Grids with adhered vesicles were rinsed with double-distilled water, stained with 2% uranyl acetate, and air dried. Finally, the samples were examined in a JEM1010 (Jeol) electron microscope operating at 80 kV. Pictures were taken with a F416TemCam

(TVIPS) CMOS camera. TEM images were analysed with ImageJ Software.

Proteomic analysis of extracellular fractions

Vesicle samples (ranging from 35 to 56 μg ml^{-1} of protein) in approximately 200 μl of TEAB 0.5 M pH 8 were resuspended in 100 μl of urea 12M to solubilize better the proteins and proceed to the digestion with trypsin in solution. Samples of the VF fractions (ranging from 240–484 μg ml^{-1} of protein) in approximately 1 ml of synthetic must pH 3.3 were evaporated to about 300 μl in a vacuum centrifuge (SpeedVac, Savant). Then, 200 μl of urea 12M was added to completely resuspend the samples, and 500 μl of each of the VF samples was loaded in a concentrator gel (stacking gel) for cleaning, before digestion with trypsin in gel. The stacking gel is a discontinuous SDS-PAGE gel with a portion of 4% concentrating gel followed by 10% separator gel. The electrophoresis stopped when the front was about 3 mm from the beginning of the separating gel. The sample band corresponding to proteins without separating was visualized with colloidal Coomassie stain and trimmed for later gel digestion.

The proteins of the VF samples present in the band of the concentrating gels were digested with trypsin. For this, the proteins were reduced with 10 mM DTT at 56°C for 30 min and then alkylated with 55 mM IA for 20 min in the dark. Finally, recombinant trypsin sequencing grade in 25 mM ammonium bicarbonate (pH 8.5) was added at a 1/20 w/w ratio to each of the VF samples and incubated overnight at 37°C. Peptide extraction was performed with 80% ACN, 0.1% TFA for 15 min for each sample, and these samples were combined with the crude obtained from each. The proteins in solution of the EV samples were reduced with 10 mM DTT for 1 h at 37°C and then alkylated with 55 mM IA for 1 h in the dark at room temperature. They were diluted with 0.5 M TEAB to be below 2 M urea, the pH was checked (pH 8), and recombinant trypsin was added to each of the samples, in the same ratio as in gel digestion, 1/20 w/w. The samples were incubated overnight.

The peptides obtained in each digestion were desalted and concentrated by pointed C18 reverse-phase chromatography (ZipTip Merck Millipore and OMIX C18 Agilent) following the manufacturer's instructions. The eluted peptides were dried by vacuum centrifugation, and the vesicle samples were reconstituted in 12 μl, while the VF-enriched fraction of *S. cerevisiae* and the VF-enriched fraction of *T. delbrueckii* were reconstituted in 15 μl and 30 μl of 2% ACN, 0.1% FA, respectively.

The sample peptides were quantified in a Qubit 3.0 fluorometer (Thermo Fischer Scientific) prior to analysis by LC-MS/MS, to inject approximately the same amount of all samples (1μg), and were frozen at −20°C until analysis. In the case of EV-enriched fractions, the quantity of peptides was out of range and the entire sample was injected.

The desalted digested proteins were analysed by RP-LC-ESI-MS/MS in an EASY-nLC 1000 System coupled to the Q-Exactive HF mass spectrometer through the Nano-Easy spray source (Thermo Fisher Scientific). Peptides were loaded onto an Acclaim PepMap 100 Trapping column (Thermo Fisher Scientific, 20 mm × 75 μm ID, 3 μm C18 resin with 100 Å pore size) using buffer A (mobile phase A: 2% AN, 0.1% FA) and then were separated and eluted on a C18 resin analytical column NTCC (Nikkyo Technos de 150 mm × 75 μm ID, 3 μm C18 resin with 100 Å pore size) with an integrated spray tip. A gradient of 5% to 30% Buffer B (100% AN, 0.1% FA) in Buffer A in 150 min at a constant flow rate of 250 nl min^{-1} was used. Data acquisition was performed with a Q-Exactive HF hybrid quadrupole-Orbitrap mass spectrometer (Thermo Fisher Scientific). Data were acquired using an ion spray voltage 1.8 kV and ion transfer temperature of 250°C. All data were acquired in a Full-MS data-dependent acquisition (DDA) in positive mode with Xcalibur 4.1 software. DDA method selected top 10 most abundant precursors with charges of 2–4 in MS 1 scans for higher energy collisional dissociation (HCD) fragmentation with a dynamic exclusion of 20 s. The MS1 scans were acquired at m/z range of 350–1700 Da with mass resolution of 60000 and automatic gain control (AGC) target of 3E^6 at a maximum Ion Time (ITmax) of 50 ms. The threshold to trigger MS2 scans was 1E^3; the normalized collision energy (NCE) was 20%; and the resolved fragments were scanned at mass resolution of 30000 and AGC target value of 2E^5 in an ITmax of 100 ms.

The MS/MS data acquired in the Q-Exactive HF were carried out using Proteome Discoverer software v.2.2 (Thermo Fisher Scientific) with search engine MASCOT 2.6 (Matrix Science, London, UK) to identify the peptides against in home-made databases with the FASTA sequence of *S. cerevisiae* downloaded from Uniprot.org (6049 sequences) and *T. delbrueckii* from NCBI (10165 sequences), a contaminant data Base (247 sequence) and Swiss-Prot (558 898 sequences). The searches were performed assuming trypsin digestion with up to 2 missed cleavage allowed, a fragment ion mass tolerance of 0.02 Da and an ion precursor tolerance of 10 ppm. Carbamidomethyl cysteine was specified as fixed modification and acetyl N-terminal, methyl loss plus acetyl N-terminal and oxidation of methionine as variable modifications. The acceptances criteria for proteins identification were an FDR < 1 %, and at least one unique peptide identified with high confidence (CI > 95%, $P < 0.05$). NSAF values were calculated, according to Zybailov *et al*. (2007).

Protein raw data were filtered, and only proteins identified in at least two of the three replicates with more than two peptides in one of the them were further considered. Comparative analysis was done based on orthologues between *S. cerevisiae* and *T. delbrueckii*. Although for most proteins there are well-identified orthologs between both yeasts, in some cases more than one protein showed high similarity. This was especially true for cell-wall- or membrane-related proteins, both categories enriched in our data sets. This was considered when comparing total number of proteins. GO enrichment and interaction networks of protein data sets were analysed using the STRING database (https://string-db.org/), respectively. Signal peptides for secretion and GPI anchor signals were predicted with SignalP4.1 (http://www.cbs.dtu.dk/services/SignalP) and PredGPI (http://gpcr.biocomp.unibo.it/predgpi/pred.htm) algorithms, respectively. Venn diagrams were done by using Venny 2.1.0 online tool software (http://bioinfogp.cnb.csic.es/tools/venny) (Oliveros, 2007–2015) and RStudio (Rstudio Team, 2015).

SDS-PAGE and peptide fingerprinting analysis of single proteins

About 10–20 μl of each EV- and VF-enriched fractions (variable protein concentration) were denatured for 5 min at 100°C in a buffer containing 125 mM Tris-HCl pH 6.8, 4% sodium dodecyl sulfate (SDS), 20% glycerol, 0.004% w/v bromophenol blue and 10% β-mercaptoethanol. Protein samples were separated by 10% SDS–polyacrylamide gel electrophoresis using the Mini-PROTEAN II electrophoresis system (Bio-Rad) according to Laemmli (1970). Gels were stained with Coomassie blue or silver staining (Pierce Silver Stain Kit; Thermo Fisher Scientific). The unstained broad range SDS-PAGE standard (#161-0317, Bio-Rad) and the prestained broad range SDS-PAGE standard (#161-0318, Bio-Rad) were used for the Coomassie blue and for the silver staining gels, respectively.

Protein bands were excised from Coomassie stained gels to carry out in-gel trypsin digestion. Briefly, band of proteins were in-gel reduced with 1,4-dithiothreitol (DTT), alkylated with iodoacetamide (IA) and digested with a 1/20 (w/w) ratio of trypsin sequencing grade (Roche Molecular Biochemicals) at 37°C, according to Sechi and Chait (1998). The peptides from proteins digested were desalted and concentrated with C18 reverse phase chromatography (OMIX C18, Agilent technologies) and the peptides were eluted with 80% acetonitrile (ACN)/0.1% trifluoroacetic acid (TFA). Finally, the samples were freeze-dried in SpeedVac, resuspended in 2% acetonitrile (AN), 0.1% formic acid (FA), and stored at −20°C until Nano LC-MS/MS analysis.

Protein identification was carried out using search engine MASCOT 2.3.0 with Proteome Discoverer software version 1.4.1.14 (Thermo Fisher Scientific) used for whole proteomic analysis. A database search was performed against *T. delbruekii* NCBI: ASM24337v1; *S. cerevisiae* NCBI: PRJNA128, PRJNA43747; and *L. thermotolerans* NCBI: PRJNA39575, PRJNA12499. Search parameters were oxidized methionine as variable modification, carbamidomethyl cysteine as fixed modification, peptide mass tolerance 9 ppm, 1 missed trypsin cleavage site and MS/MS fragment mass tolerance of 0.8 Da. In all protein identification, the false discovery rate (FDR) was $< 1\%$, using a Mascot Percolator, with a *q*-value of 0.01.

EXG1 knock-out and activity assays

A disruption cassette was obtained by PCR amplification of plasmid pYM39 (Euroscarf), in two steps, first with primers 5′-CAGCTCTAGTACGTCACAGAGGGATCCGCTAGGGATAACAGG-3′ and 5′- GGCCTGGATATTGTCTTGCGGCATCGATGAATTCGAGCTCG -3′, and then with primers 5′-TTTTCATTTAGTAGTTTTTGAGATCTGTTTCAGCTCTAGTACGTCACAGAGG-3′ and 5′-CTATAAGGGCGATTTGAAATCAGTTACATTGGCCTGGATATTGTCTTGCGG-3′. The final amplification product (1533 bp) contained the KanMX selection marker, flanked by *Ashbya gossypii* TEF promoter and terminator sequences, and 50 bp overhangs to drive recombination to replace the Tdel_0G03720 ORF (homologous to *S. cerevisiae EXG1*). *T. delbrueckii* was transformed with this construction as described by Gietz and Woods (2002) but the thermal shock was at 42°C for 40 min. Transformants were selected at 25°C, 48–72 h in YPD plates supplemented with 200 μg ml^{-1} G418. Homologous recombination was confirmed by PCR amplification with primers 5′-GCTTCACTACGAGATACCGACG-3′ and 5′-GTACGGGCGACAGTCACATCAT-3′, targeting the 5′ insertion edge; and 5′-GTTTTTGCGTCTTAGCATCTAGA-3′ and 5′-ATGGTCGGTACGCTCACAGCAT-3′, for the whole region. Deletion was further confirmed by a silver-stained 10% SDS-PAGE gel, performed as described above, containing 20 μl of the 0.22 μm filtered 24-h cell-free supernatants of *T. delbrueckii* wild-type and knock-out strains, and by the loss of hydrolytic activity with 5 μl of the same cell-free supernatants. The hydrolysis assay was performed in a final volume of 50 μl, 4 mM p-Nitrophenyl β-D-glucopyranoside and 0.1 M NaOAc pH 5.5. The samples were incubated at 37°C for 6 h. The reaction was terminated with 100 μl 1 M Na_2CO_3. The A_{405} of the samples was determined in a microplate reader (SPECTROstar Nano, BMG LABTECH).

Biological activity assay

Yeast growth in MS300 was performed at 25°C in fully independent triplicates in 96-well microplates, without stirring. Cultures were inoculated to 0.1 initial OD_{600}, in a final volume of 200 μl. Treatments with 0.22 μm filtered 24-h cell-free supernatants from *S. cerevisiae* (FX10 and EC1118), *T. delbrueckii* (PR678 and PRICVV collection*) and L. thermotolerans* were performed with 50 μl. Samples were taken at the indicated times (see Results). Living and dead cells were quantified by flow cytometry using a CytoFLEX Flow Cytometer (Beckman Coulter) using the cell-impermeant dye SYTOX™ Green Dead Cell (Thermo Fisher Scientific). Dye was diluted (1/200) in 0.1 M pH 8 Tris-HCl buffer from a 40 μM frozen stock, and 200 μl of it was combined with 50 μl of sample (direct or 1:10 diluted). Samples were analysed with a sample flow rate of 10 μl ml^{-1}, and 60 s recording time, with automatic threshold in FSC channel. The detection channels were FITC-A for living cells, and PC5.5-A for dead cells.

Statistical analysis

Average values from flow cytometry analyses were compared by one-way analysis of variance (ANOVA), with Dunnett's (bilateral) test, with a level of significance $\alpha = 0.05$. All analyses were performed using SPSS Statistics v. 25 software (IBM, Armonk, NY, USA).

Acknowledgements

This work was funded by the Spanish Government through grants AGL2015-63629-R (co-financed by FEDER funds), PCI2018-092949 (co-funded by ERA-CoBioTech) and BES-2016-077557 (training contract for AM). JT is funded by FGCSIC by the COMFUTURO program. The authors would like to thank Cristina Juez and Laura López for technical assistance, Fernanda Ruiz for help with ultracentrifugation, María Teresa Rejas for her support with the TEM analysis, and Concha Gil and Lola Gutiérrez for advice on sample processing for proteomics.

Conflict of interest

None declared.

Author contribution

RG and PM conceptualized and designed the project. AM, EV, PM and JT performed the experimental work. AM and JT performed data analysis. RG, PM, JT, AM and KRP interpreted results. RG and AM wrote the article. All the authors reviewed and approved the manuscript.

References

Alonso del Real, J., Pérez-Torrado, R., Querol, A., and Barrio, E. (2019) Dominance of wine *Saccharomyces cerevisiae* strains over *S. kudriavzevii* in industrial fermentation competitions is related to an acceleration of nutrient uptake and utilization. *Environ Microbiol* **21:** 1627–1644.

Baltazar, M.L., Nakayasu, E.S., Sobreira, T.J., Choi, H., Casadevall, A., Nimrichter, L., *et al*. (2016) Antibody binding alters the characteristics and contents of extracellular vesicles released by *Histoplasma capsulatum*. *mSphere* **1:** e00085-15.

Bely, M., Sablayrolles, J., and Barré, P. (1990) Automatic detection of assimilable nitrogen deficiencies during alcoholic fermentation in oenological conditions. *J Ferment Bioengineer* **70:** 246–252.

Bhatnagar, S., Shinagawa, K., Castellino, F.J., and Schorey, J.S. (2007) Exosomes released from macrophages infected with intracellular pathogens stimulate a proinflammatory response in vitro and in vivo. *Blood* **110:** 3234–3244.

Branco, P., Francisco, D., Chambon, C., Hébraud, M., Arneborg, N., Almeida, M.G., *et al*. (2014) Identification of novel GAPDH-derived antimicrobial peptides secreted by *Saccharomyces cerevisiae* and involved in wine microbial interactions. *Appl Microbiol Biotechnol* **98:** 843–853.

Brown, L., Wolf, J.M., Prados-Rosales, R., and Casadevall, A. (2015) Through the wall: extracellular vesicles in Gram-positive bacteria, mycobacteria and fungi. *Nat Rev Microbiol* **13:** 620–630.

Chen, H., and Fink, G.R. (2006) Feedback control of morphogenesis in fungi by aromatic alcohols. *Genes Dev* **20:** 1150–1161.

Chen, H., Fujita, M., Feng, Q., Clardy, J., and Fink, G.R. (2004) Tyrosol is a quorum-sensing molecule in *Candida albicans*. *Proc Natl Acad Sci* **101:** 5048–5052.

Curiel, J.A., Morales, P., Gonzalez, R., and Tronchoni, J. (2017) Different non-*Saccharomyces* yeast species stimulate nutrient consumption in *S. cerevisiae* mixed cultures. *Front Microbiol* **8:** 2121.

De Vuyst, L., Van Kerrebroeck, S., Harth, H., Huys, G., Daniel, H.M., and Weckx, S. (2014) Microbial ecology of sourdough fermentations: diverse or uniform? *Food Microbiol* **37:** 11–29.

Decker, B.L., and Wickner, W.T. (2006) Enolase activates homotypic vacuole fusion and protein transport to the vacuole in yeast. *J Biol Chem* **281:** 14523–14528.

Ene, I.V., Walker, L.A., Schiavone, M., Lee, K.K., Martin-Yken, H., Dague, E., *et al*. (2015) Cell wall remodeling enzymes modulate fungal cell wall elasticity and osmotic stress resistance. *MBio* **6:** e00986-15.

Englezos, V., Rantsiou, K., Giacosa, S., Río Segade, S., Rolle, L., and Cocolin, L. (2019) Cell-to-cell contact mechanism modulates *Starmerella bacillaris* death in mixed culture fermentations with *Saccharomyces cerevisiae*. *Int J Food Microbiol* **289:** 106–114.

Farnworth, E.R. (2005) Kefir—a complex probiotic. *Food Sci Technol Bull* **2:** 1–17.

Fleet, G.H. (2003) Yeast interactions and wine flavour. *Int J Food Microbiol* **86:** 11–22.

Fonseca, P., Vardaki, I., Occhionero, A., and Panaretakis, T. (2016) Metabolic and signaling functions of cancer cell-derived extracellular vesicles. *Int Rev Cell Mol Biol* **326:** 175–199.

Furukawa, S., Watanabe, T., Toyama, H., and Morinaga, Y. (2013) Significance of microbial symbiotic coexistence in traditional fermentation. *J Biosci Bioeng* **116:** 533–539.

Gancedo, C., and Flores, C.L. (2008) Moonlighting proteins in yeasts. *Microbiol Mol Biol Rev* **72:** 197–210.

Gietz, R.D., and Woods, R.A. (2002) Transformation of yeast by lithium acetate/single-stranded carrier DNA/polyethylene glycol method. *Methods Enzymol* **350:** 87–96.

Gil-Bona, A., Llama-Palacios, A., Parra, C.M., Vivanco, F., Nombela, C., Monteoliva, L., *et al*. (2015) Proteomics unravels extracellular vesicles as carriers of classical cytoplasmic proteins in *Candida albicans*. *J Proteome Res* **14:** 142–153.

Gil-Bona, A., Amador-García, A., Gil, C., and Monteoliva, L. (2017) The external face of *Candida albicans*: a proteomic view of the cell surface and the extracellular environment. *J Proteomics* **180:** 70–79.

Gonzalez, R., Quirós, M., and Morales, P. (2013) Yeast respiration of sugars by non-*Saccharomyces* yeast species: a promising and barely explored approach to lowering alcohol content of wines. *Trends Food Sci Technol* **29:** 55–61.

González, B., Vázquez, J., Cullen, P.J., Mas, A., Beltran, G., and Torija, M.-J. (2018) Aromatic amino acid-derived compounds induce morphological changes and modulate the cell growth of wine yeast species. *Front Microbiol* **9:** 670.

Hong, J., Dauros-Singorenko, P., Whitcombe, A., Payne, L., Blenkiron, C., Phillips, A., *et al*. (2019) Analysis of the *Escherichia coli* extracellular vesicle proteome identifies markers of purity and culture conditions. *J Extracell Vesicles* **8:** 1632099.

Jiang, C., Song, J., Cong, H., Zhang, J., and Yang, Q. (2017) Expression and characterization of a novel antifungal exo-β-1,3-glucanase from *Chaetomium cupreum*. *Appl Biochem Biotechnol* **182:** 261–275.

Jolly, N.P., Varela, C., and Pretorius, I.S. (2014) Not your ordinary yeast: non-*Saccharomyces* yeasts in wine production uncovered. *FEMS Yeast Res* **14:** 215–237.

Jouhten, P., Ponomarova, O., Gonzalez, R., and Patil, K.R. (2016) *Saccharomyces cerevisiae* metabolism in ecological context. *FEMS Yeast Res* **16:** fow080.

Kunkee, R.E. (1984) Selection and modification of yeasts and lactic acid bacteria for wine fermentation. *Food Microbiol* **1:** 315–332.

Laemmli, U.K. (1970) Cleavage of structural proteins during the assembly of the head of bacteriophage T4. *Nature* **227:** 680–685.

Manzanares, P., Valles, S., and Viana, F. (2011) Non-*Saccharomyces* yeasts in the winemaking process. In *Molecular Wine Microbiology*. Carrascosa, A., Muñoz, R., and Gonzalez, R. (eds). Ansterdam: Academic Press, pp. 85–110.

Marzesco, A.M., Janich, P., Wilsch-Bräuninger, M., Dubreuil, V., Langenfeld, K., Corbeil, D., and Hutter, W.B. (2005) Release of extracellular membrane particles carrying the stem cell marker prominin-1 (CD133) from neural progenitors and other epithelial cells. *J Cell Sci* **118:** 2849–2858.

Miura, N., and Ueda, M. (2018) Evaluation of unconventional protein secretion by *Saccharomyces cerevisiae* and other fungi. *Cells* **7:** 128.

Miura, N., Kirino, A., Endo, S., Morisaka, H., Kuroda, K., Takagi, M., *et al*. (2012) Tracing putative trafficking of the glycolytic enzyme enolase via SNARE-driven unconventional secretion. *Eukaryot Cell* **11:** 1075–1082.

Nickel, W., and Rabouille, C. (2009) Mechanisms of regulated unconventional protein secretion. *Nat Rev Mol Cell Biol* **10:** 148–155.

Oliveira, D.L., Nakayasu, E.S., Joffe, L.S., Guimarães, A.J., Sobreira, T.J.P., Nosanchuk, J.D., *et al*. (2010) Characterization of yeast extracellular vesicles: evidence for the participation of different pathways of cellular traffic in vesicle biogenesis. *PLoS One* **5:** e11113.

Oliveira, D.L., Rizzo, J., Joffe, L.S., Godinho, R.M.C., and Rodrigues, M.L. (2013) Where do they come from and where do they go: Candidates for regulating extracellular vesicle formation in fungi. *Int J Mol Sci* **14:** 9581–9603.

Oliveros, J.C. (2007–2015) Venny. An interactive tool for comparing lists with Venn's diagrams. URL http://bioinfogp.cnb.csic.es/tools/venny/index.html.

Park, J.E., Tan, H.S., Datta, A., Lai, R.C., Zhang, H., Meng, W., *et al*. (2010) Hypoxic tumor cell modulates its microenvironment to enhance angiogenic and metastatic potential by secretion of proteins and exosomes. *Mol Cell Proteomics* **9:** 1085–1099.

Peres da Silva, R., Puccia, R., Rodrigues, M.L., Oliveira, D.L., Joffe, L.S., César, G.V., *et al*. (2015) Extracellular vesicle-mediated export of fungal RNA. *Sci Rep* **5:** 7763.

Pérez, F., Ramírez, M., and Regodón, J.A. (2001) Influence of killer strains of *Saccharomyces cerevisiae* on wine fermentation. *Antonie van Leeuwenhoek, Int J Gen Mol Microbiol* **79:** 393–399.

Pérez-Torrado, R., Rantsiou, K., Perrone, B., Navarro-Tapia, E., Querol, A., and Cocolin, L. (2017) Ecological interactions among *Saccharomyces cerevisiae* strains: insight into the dominance phenomenon. *Sci Rep* **7:** 43603.

Rabouille, C., Malhotra, V., and Nickel, W. (2012) Diversity in unconventional protein secretion. *J Cell Sci* **125:** 5251–5255.

Raposo, G., and Stahl, P.D. (2019) Extracellular vesicles: a new communication paradigm? *Nat Rev Mol Cell Biol* **20:** 509–510.

Raposo, G., Nijman, H.W., Stoorvogel, W., Liejendekker, R., Harding, C.V., Melief, C.J., and Geuze, H.J. (1996) B lymphocytes secrete antigen-presenting vesicles. *J Exp Med* **183:** 1161–1172.

Regente, M., Corti-Monzón, G., Maldonado, A.M., Pinedo, M., Jorrín, L., and de la Canal, J. (2009) Vesicular fractions of sunflower apoplastic fluids are associated with potential exosome marker proteins. *FEBS Lett* **583:** 3363–3366.

Rizzo, J., Nimrichter, L., and Rodrigues, M.L. (2017) What is new? Recent knowledge on fungal extracellular vesicles. *Curr Fungal Infect Rep* **11:** 141–147.

Rodrigues, M.L., and Casadevall, A. (2018) A two-way road: novel roles for fungal extracellular vesicles. *Mol Microbiol* **110:** 11–15.

Rodrigues, M.L., Nimrichter, L., Oliveira, D.L., Frases, S., Miranda, K., Zaragoza, O., *et al*. (2007) Vesicular polysaccharide export in *Cryptococcus neoformans* is a eukaryotic solution to the problem of fungal trans-cell wall transport. *Eukaryot Cell* **6:** 48–59.

Rodrigues, M.L., Nakayasu, E.S., Almeida, I.C., and Nimrichter, L. (2014) The impact of proteomics on the understanding of functions and biogenesis of fungal extracellular vesicles. *J Proteomics* **31:** 177–186.

Rodríguez-Cousiño, N., Maqueda, M., Ambrona, J., Zamora, E., Esteban, R., and Ramírez, M. (2011) A new wine *Saccharomyces cerevisiae* killer toxin (Klus), encoded by a double-stranded RNA virus, with broad antifungal activity is evolutionarily related to a chromosomal host gene. *Appl Environ Microbiol* **77:** 1822–1832.

Rossouw, D., Meiring, S.P., and Bauer, F.F. (2018) Modifying Saccharomyces cerevisiae adhesion properties regulates yeast ecosystem dynamics. *mSphere* **3:** e00383-18.

RStudio Team (2015) *RStudio: Integrated Development for R*. Boston, MA: RStudio. URL http://www.rstudio.com/.

Schaeffer, H.J., Leykam, J., and Walton, J.D. (1994) Cloning and targeted gene disruption of *EXG1*, encoding exo-beta 1,3-glucanase, in the phytopathogenic fungus *Cochliobolus carbonum*. *Appl Environ Microbiol* **60:** 594–598.

Sechi, S., and Chait, B.T. (1998) Modification of cysteine residues by alkylation. A tool in peptide mapping and protein identification. *Anal Chem* **70:** 5150–5158.

Shekhawat, K., Patterton, H., Bauer, F.F., and Setati, M.E. (2019) RNA-seq based transcriptional analysis of *Saccharomyces cerevisiae* and *Lachancea thermotolerans* in mixed-culture fermentations under anaerobic conditions. *BMC Genom* **20:** 145.

Stahl, P.D., and Raposo, G. (2018) Exosomes and extracellular vesicles: the path forward. *Essays Biochem* **62:** 119–124.

Taillandier, P., Lai, Q.P., Julien-Ortiz, A., and Brandam, C. (2014) Interactions between *Torulaspora delbrueckii* and *Saccharomyces cerevisiae* in wine fermentation: influence of inoculation and nitrogen content. *World J Microbiol Biotechnol* **30:** 1959–1967.

Théry, C., Witwer, K.W., Aikawa, E., Alcaraz, M.J., Anderson, J.D., Andriantsitohaina, R., *et al*. (2018) Minimal information for studies of extracellular vesicles 2018 (MISEV2018): a position statement of the International Society for Extracellular Vesicles and update of the MISEV2014 guidelines. *J Extracell Vesicles* **7:** 1535750.

Tronchoni, J., Curiel, J.A., Morales, P., Torres-Pérez, R., and Gonzalez, R. (2017) Early transcriptional response to biotic stress in mixed starter fermentations involving *Saccharomyces cerevisiae* and *Torulaspora delbrueckii*. *Int J Food Microbiol* **241:** 60–68.

Vallejo, M.C., Nakayasu, E.S., Matsuo, A.L., Sobreira, T.J., Longo, L.V., Ganiko, L., *et al*. (2012) Vesicle and vesicle-free extracellular proteome of *Paracoccidioides brasiliensis*: comparative analysis with other pathogenic fungi. *J Proteome Res* **11:** 1676–1685.

Van Vuuren, H.J.J., and Jacobs, C.J. (1992) Killer yeasts in the wine industry: a review. *Am J Enol Vitic* **43:** 119–128.

Vargas, G., Rocha, J.D., Oliveira, D.L., Albuquerque, P.C., Frases, S., Santos, S.S., *et al*. (2015) Compositional and immunobiological analyses of extracellular vesicles released by *Candida albicans*. *Cell Microbiol* **17:** 389–407.

Velázquez, R., Zamora, E., Álvarez, M.L., Hernández, L.M., and Ramírez, M. (2015) Effects of new *Torulaspora delbrueckii* killer yeasts on the must fermentation kinetics and aroma compounds of white table wine. *Front Microbiol* **6:** 1222.

Wang, C., Mas, A., and Esteve-Zarzoso, B. (2015) Interaction between *Hanseniaspora uvarum* and *Saccharomyces cerevisiae* during alcoholic fermentation. *Int J Food Microbiol* **206:** 67–74.

Winters, C.M., Hong-Brown, L.Q., and Hui-Ling, C. (2020) Intracellular vesicle clusters are organelles that synthesize extracellular vesicle-associated cargo proteins in yeast. *J Biol Chem* **295:** 2650–2663.

Wolf, J.M., and Casadevall, A. (2014) Challenges posed by extracellular vesicles from eukaryotic microbes. *Curr Opin Microbiol* **22:** 73–78.

Zhao, K., Bleackley, M., Chisanga, D., Gangoda, L., Fonseka, P., Liem, M., *et al*. (2019) Extracellular vesicles secreted by *Saccharomyces cerevisiae* are involved in cell wall remodelling. *Commun Biol* **2:** 305.

Zybailov, B.L., Florens, L., and Washburn, M.P. (2007) Quantitative shotgun proteomics using a protease with broad specificity and normalized spectral abundance factors. *Mol Biosyst* **3:** 354–360.

Supporting information

Additional supporting information may be found online in the Supporting Information section at the end of the article.

Fig. S1. Box plot showing normalized relative spectral abundance factor (NSAF) of the 22 most abundant proteins in *S. cerevisiae* and *T. delbrueckii* VF and EV-enriched fractions. Data from three biological replicates are presented.

Fig. S2. Coomassie Blue stained SDS-PAGE gels of proteins from extracellular fractions from different wine yeast strains. EV: EV-enriched fraction; FT: Flow-through; RT: Retentate (both FT and RT contribute to the VF-enriched fraction; see Experimental procedures). Size of bands from the molecular weight marker, in KDa, are shown to the left of each gel.

Fig. S3. Box plot showing mortality of *S. cerevisiae* FX10 induced by different cell-free supernatants of *T. delbrueckii* strains. Confidence bars represent standard deviation measures. Data from three biological replicates are presented. Statistically significant differences with the PBS control, within each time point, are indicated by * or *** for *P*-values ≤ 0.05 or ≤ 0.001, respectively.

Fig. S4. Silver-stained SDS-PAGE confirming the absence of Exg1 (50 KDa approx. band) in the cell-free supernatants of two knock-out selected strains compared to the original strain of *T. delbrueckii* (A), and β-glucosidase activity assay

confirming lack of β-glucanase enzymatic activity on the same samples (B).

Table S1. NSAF values for proteins identified in at least 2 replicates with more than 2 peptides in one of them in each of four data sets (EV-enriched fraction, and VF-enriched fraction for both *T. delbrueckii* and *S. cerevisiae*). Additional information includes cellular categorization as described in the manuscript, presence of signal peptide processing signals, and presence of GPI-anchor signals.

Table S2. GO enrichment analysis of the proteins present in VF- and EV-enriched fraction of *S. cerevisiae* (*Sc*), *T. delbrueckii* (*Td*) separately and in common between the fractions of the different yeasts. Categories mentioned verbatim in the manuscript are highlighted in read.

